J. Am. Chem. Soc. **1995,** *117,* 11407−11420

Photophysics of Poly(paracyclophan-1-ene) and Derivatives: Evidence for Intrachain Energy Transfer and Chromophore Aggregation

Yi-Jun Miao, William G. Herkstroeter, Benjamin J. Sun, Antek G. Wong-Foy, and Guillermo C. Bazan*

Contribution from the Department of Chemistry, University of Rochester, Rochester, New York 14627

Received June 2, 1995[⊗]

Abstract: The monomer [2.2]paracyclophan-1-ene (**2**) reacts with the Schrock initiator $Mo(NAr)(OC(CF_3)_2Me)_2(CHCMe_2Ph)$ (**1**, Ar = 2,6-diisopropylphenyl), via a living and *cis*-specific ring-opening metathesis polymerization (ROMP) mechanism, to give poly**2** in essentially quantitative yield. This polymerization is significantly slower than those observed with monomers built on the norbornene skeleton. The monomers 9-[(*tert*-butyldimethylsilyl)oxy][2.2]paracyclophan-1-ene (**3**) and 9-(*n*-butyl)-9-[(*tert*-butyldimethylsilyl)oxy][2.2]paracyclophan-1-ene (**4**) react similarly, but the resulting polymers are significantly more soluble as a result of the increased saturated content of the polymer chain. Depending on the manner of monomer addition, it is possible to prepare either random or block copolymers (of narrow polydispersity). Poly**2**, poly**3**, and poly**4** obtained with **1** are stereoregular main-chain polystilbenes with close structural links to poly(*p*-phenylenevinylene). Poly**2** and poly**3** in particular have a strong, vibronically defined, red-shifted component in their photoluminescence spectra which depends strongly on the polymer stereochemistry, proximity of chromophores, backbone substitution, ability of the medium to solvate the polymer coils, and length of the stilbene-containing segments. These data suggest that chromophore cooperativity, or aggregation, is responsible for the lower energy fluorescence band. Fluorescence depolarization and lifetime measurements are consistent with significant energy transfer from excited monomeric stilbenes to "aggregated" sites. Poly**4** is sufficiently substituted that chromophore cooperativity is observed only in the film state and in poor solvents which contract coil dimensions. The oxidative photocyclization of the stilbene components to phenanthrene (poly**5**) proceeds quantitatively using iodine and a large excess of propylene oxide. This structural change causes a significant decrease in the polymer's hydrodynamic volume, and importantly, no evidence of chromophore cooperativity has been observed in poly**5**.

Introduction

Nonconjugated polychromophores often display complex physical behavior different from that expected in a collection of noninteracting chromophores.[1] This class of macromolecules has been studied intensely for their potential use in long distance electron and energy transfer, *i.e.*, "photon-harvesting" polymers.[2] As a result of the geometrical constraints implicit in leashing chromophores in a regular and alternating sequence, the emissive relaxation after photoexcitation may involve more than one species and is often observed as excited dimer (excimer) fluorescence.[1a,3] The extent to which excimer emission dominates over normal monomer emission depends strongly on the proximal distance between chromophores. The most intensely studied polymers contain the photoactive species pendant to the backbone in well-defined three-carbon repeating intervals and can be readily obtained from simple free radical polymerization of vinyl monomers with polynuclear aromatic chromophores such as phenyl, pyrenyl, naphthyl, anthryl, etc.[4]

Aromatic polychromophores wherein the functionalities are integral to backbone composition and are separated by a short saturated tether (link with three atoms or less) have received less attention than their pendant counterparts. Two factors may account for this bias. First, their preparation has previously relied on synthetically more stringent step-growth methods.[5] Second, to improve solubility, it is usually necessary to incorporate a long flexible link between chromophores or to attach substituents that minimize interchain interactions. However, modifications that improve solubility dilute the chromophores within the polymer and ultimately diminish their ability to interact with each other. Photochemical studies and structural analysis of main-chain polychromophores are of interest, especially in cases where photoactive species comprise a large percentage of the total polymer mass since, relative to their pendant counterparts, cooperativity should show enhanced sensitivity to chain dynamics and secondary structure.

There exists ample documentation of rapid singlet energy migration and charge separation in polychromophores.[6] The distances spanned are greater than two chromophores, and migration may proceed either in a systematic linear motion along the backbone or across nonvicinal chromophores which are brought into close proximity as a result of chain folding or dynamics. More than one mechanism of transfer has been shown to be operative within single chains.[7] Additionally, although the effective local concentration of chromophores

---

[⊗] Abstract published in *Advance ACS Abstracts,* November 1, 1995.

[1] (a) *Photophysics of Polymers*; Hoyle, C. E., Torkelson, J. M. Eds.; ACS Symposium Series 358; American Chemical Society: Washington, DC, 1987. (b) Winnik, F. M. *Chem. Rev.* **1993**, *93*, 587.

[2] (a) Watkins, D. M.; Fox, M. A. *J. Am. Chem. Soc.* **1994**, *116*, 6441. (b) Jones, W. E.; Baxter, S. M.; Strouse, G. F.; Meyer, T. J. *J. Am. Chem. Soc.* **1994**, *115*, 6441.

[3] Guillet, Je. *Polymer Photophysics and Photochemistry*; Cambridge University Press: Cambridge, U.K. 1985.

[4] Kalyanasundaram, K. *Photochemistry in Microheterogeneous Systems*; Academic Press: New York, 1987.

[5] See, for example, Yang, Z.; Sokolik, I.; Karasz, F. E. *Macromolecules* **1993**, *26*, 1188.

[6] Webber, S. E. *Chem. Rev.* **1990**, *90*, 1469 and references therein.

[7] Guillet, J. E. *Polym. Prepr.* (*Am. Chem. Soc., Div. Polym. Chem.*) **1979**, *20*, 395.

0002-7863/95/1517-11407$09.00/0

remains constant upon dilution, there is a strong dependence on solvent. Chains dissolved in a good solvent have extended configurations with an interchromophore average distance larger than in contracted coils surrounded by a poor solvent. Parameters, such as molecular weight, tacticity (stereoregularity), concentration, and temperature, which control the efficiency of energy transfer, also affect excimer formation. This complex interdependence, together with difficulties in direct experimental access, has made controlling energy migration a difficult task despite its potential to separate charge and mimic antenna pigments in photosynthesis.

Conjugated polymers may be viewed as the extreme of main-chain polychromophores where no spacer between chromophores exists.[8] The emissive subset of this class of materials has received intense research attention recently because of its potential to serve as the emissive component in technologically relevant optoelectronic devices such as light-emitting diodes (LEDs).[9] Recent studies have shown that for certain π-conjugated polymers in thin films both the fluorescence wavelength and quantum yield are limited by excimer formation. Addition of donors to these films results in improved efficiencies because photogeneration now is exciplex-mediated.[10] Similarly, other external agents efficiently form excited state complexes after photoexcitation that lead to electron transfer.[11] Modulation of photophysical processes in this way clearly underscores the important role of supramolecular interactions between the photoactive species in these polymers and their role in improving bulk performance.

We have recently published the preparation and preliminary photophysical studies of poly(paracyclophan-1-ene). Use of the molybdenum-based Schrock alkylidene complex Mo(NAr)(OC(CF$_3$)$_2$Me)$_2$(CHCHe$_2$Ph) (**1**, Ar = 2,6-diisopropylphenyl) is central to the synthetic success of this reaction by promoting the living and *cis*-specific ring-opening metathesis polymerization (ROMP) of [2.2]paracyclophan-1-ene (**2**) (eq 1).[12] The structure of *cis*-poly**2** is aesthetically simple. It may be viewed as a stereoregular polychromophore made up of *cis*-stilbene components interconnected via ethylene linkages. These chromophores are oriented in the same direction with a strict configurational arrangement, and the percentage weight of polymer which is photoactive is higher than that of typical all-organic polychromophores. A complementary description for poly**2** can be obtained by starting with *cis*-poly(*p*-phenylenevinylene) (PPV) and selectively hydrogenating every alternate vinyl linkage. The architecture of poly(paracyclophan-1-ene) and its derivatives then serves as a bridge between conjugated emissive polymers and main-chain polychromophores. Not surprisingly then, our initial studies of poly**2** revealed a complex, irradiation dependent, photophysical behavior with features reminiscent of aggregated stilbenes.[13] Further monomer modification has also led us to 9-[(*tert*-butyldimethylsilyl)oxy][2.2]paracyclophan-1-ene (**3**) which can be polymerized to precursor materials that can be converted to fully conjugated PPV under mild conditions (eq 2).[14]

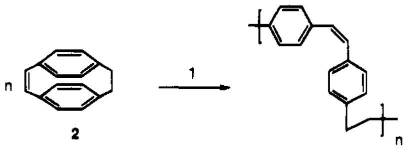

2

cis-poly-**2**

(1)

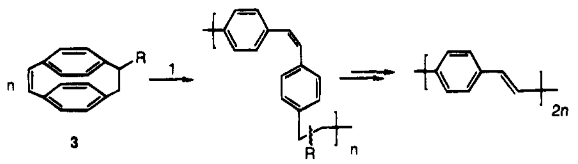

3

cis-poly-**3**

R = OSiMe$_2{}^t$Bu

(2)

We report in this paper full synthetic details for the preparation of these polymers and our studies concerning the effects of structural composition on the bulk photophysics of poly(paracyclophan-1-ene)s. We are particularly interested in designing, developing, and exploiting synthetic methodologies to prepare compounds that probe how intrachain chromophore interactions depend on secondary structure. Factors and variables that are investigated are stereoregularity, emissive segment length, chromophore density, characteristics of the constituent chromophores, and interference from polymer side groups. Results of this study are relevant to our understanding of inter- and intrachain interactions in the solid state of polychromophores and their effect on bulk performance.

Results

Synthesis of Monomers, Homopolymers, and Block Copolymers.[15] Conceptually, the monobromination of paracyclophane followed by elimination should provide a convenient source of **2**. However, selective monobromination of paracyclophane, according to the procedure of Hopf and Psiorz,[16] on a large scale (~30 g of paracyclophane) is difficult. Every attempt to scale up resulted in the desired monobrominated species being contaminated with paracyclophanes containing varying amounts of polybromination. Pure 1-bromo[2.2]paracyclophane is difficult to isolate. Our procedure was to separate the brominated products from unreacted paracyclophane by flash chromatography. The crude mixture of products was then reacted directly with potassium *tert*-butoxide from which **2** was isolated by chromatography. Problems in controlling the bromination step have been observed previously[17] and ultimately result in a low yield of **2**. Polymer preparations rely on the living and *cis*-specific ROMP of paracyclophan-1-ene and its derivatives promoted by initiator **1** (eq 1). These reactions are slow relative to polymerization of monomers built on the norbornene framework; for example, 100 equiv of [2.2]paracyclophan-1-ene (**2**) requires close to 24 h at room temperature for complete consumption using a 10^{-5} M solution of initiator. Since the ring strain of paracyclophane[18] is comparable to that of norbornene, we ascribe this attenuated reactivity to both steric congestion between the bulky substituents on the ligand sphere of molybdenum and the ortho hydrogens in the monomer and the electronic stability of the propagating benzylidene.[19] After termination with benzaldehyde, polymer samples were purified prior to photophysical studies. This

---

[8] Bredas, J. L., Silbey, R., Eds. *Conjugated Polymers: The Novel Science and Technology of Highly Conducting and Nonlinear Active Materials*; Kluwer Academic Publishers: Dordrecht, The Netherlands, 1991.

[9] Clery, D. *Science* **1994**, *263*, 1700.

[10] Jenekhe, S. A.; Osaheni, J. A. *Science* **1994**, *265*, 765.

[11] Sariciftci, N. S.; Smilowitz, L.; Heeger, A. J.; Wudl, F. *Science* **1992**, *258*, 1474.

[12] Miao, Y.-J.; Bazan, G. C. *Macromolecules* **1994**, *27*, 1063.

[13] For a recent review: Whitten, D. G. *Acc. Chem. Res.* **1993**, *26*, 502.

[14] Miao, Y.-J.; Bazan, G. C. *J. Am. Chem. Soc.* **1994**, *116*, 9379.

[15] A portion of this work has previously appeared in ref 12.

[16] Hopf, H.; Psiorz, M. *Chem. Ber.* **1986**, *119*, 1836.

[17] Reiser, O.; Konig, B.; Meerholz, K.; Heinze, J.; Welauer, T.; Gerson, F.; Frim, R.; Rabinovitz, M.; de Meijere, A. *J. Am. Chem. Soc.* **1993**, *115*, 3511.

[18] Vögtle, F. *Cyclophane Chemistry*; Wiley: New York, 1993.

[19] Schrock, R. R.; DePue, R.; Feldman, J.; Schaverien, C. J.; Dewan, J. C.; Liu, A. H. *J. Am. Chem. Soc.* **1988**, *110*, 1423.

Table 1. GPC Data for Isolated Polymers[a]

sample	$M_n{}^b$(calcd)	M_n(found)	PDI
poly$\mathbf{2}_{100}$	20 600	26 000	1.2
poly$\mathbf{3}_{100}$	33 600	26 273	1.1
poly$\mathbf{3}_{200}$	67 200	59 351	1.2
poly$\mathbf{4}_{50}$	19 800	18 400	1.2
poly$\mathbf{2}_{10}$-*block*-polyNBE$_{200}$	21 272	20 500	1.1
poly$\mathbf{3}_{5}$-*block*-polyNBE$_{150}$	15 780	17 643	1.3
poly$\mathbf{3}_{10}$-*block*-polyNBE$_{200}$	22 160	23 600	1.3
poly$\mathbf{3}_{20}$-*block*-polyNBE$_{200}$	25 520	24 100	1.3
poly$\mathbf{3}_{20}$-*block*-polyNBE$_{60}$	12 360	12 660	1.3
poly$\mathbf{4}_{50}$-*block*-polyNBE$_{10}$	29 050	36 800	1.1

[a] All GPC results are calibrated against polystyrene standards. [b] M_n = number average molecular weight.

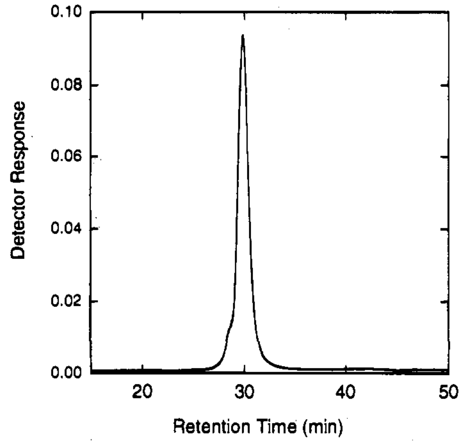

Figure 1. GPC elution curve of poly$\mathbf{2}_{10}$-*block*-polyNBE$_{200}$ in chloroform.

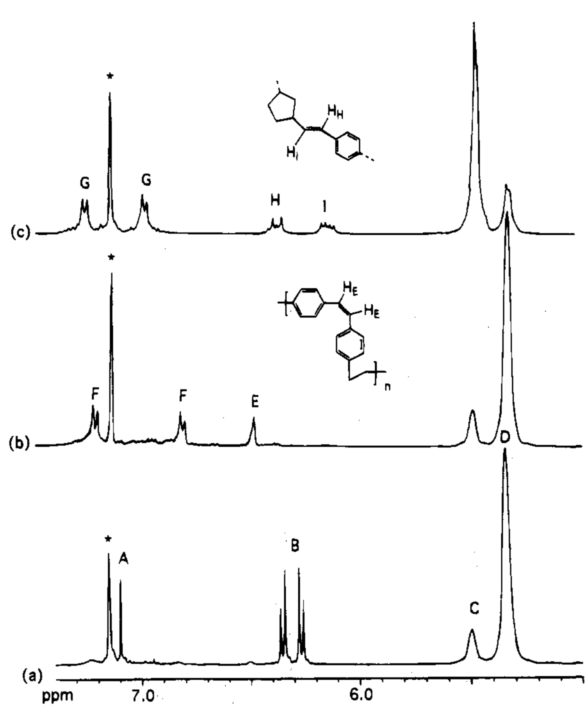

Figure 2. ^{1}H NMR spectra of the reaction resulting from the simultaneous addition of 10 equiv of **2** and 150 equiv of NBE to **1** at (a) 15 min (A and B are the olefinic and aromatic resonances of **2**, respectively, C and D are due to the *trans*- and *cis*-olefins in polyNBE$_{150}$, and the asterisk indicates C_6D_5H), (b) 4 h (E and F are the olefinic and aromatic resonances of poly**2**, respectively), and (c) 24 h (G, H, and I are due to resonances from the new *trans*-cyclopentylphenylolefin units).

purification was by triple precipitation of concentrated CH_2Cl_2 solutions of polymers into HPLC-grade pentane or, in the case of block copolymers, into methanol.

The slow rate of the propagation sequence removes some flexibility for the preparation of block copolymers because it is competitive with the rates of secondary metathesis, *i.e.*, chain transfer, observed in polynorbornenes. Thus, the order of addition is important. In order to prepare a block copolymer containing polynorbornene (polyNBE) and poly**2**, the norbornene (NBE) *must* be added to living poly**2**. For best results, the first step, polymerization of **2**, is done over a period of 24 h under vacuum using rigorously dried toluene. As is the case for all living polymerizations, extra care must be paid to the purity of the monomers, initiator, and solvents. Addition of NBE is done quickly while maximizing the efficiency and rate of stirring, and after 5−10 min the reaction is quenched with benzaldehyde. The block copolymers obtained under these conditions have narrow polydispersities (Table 1) and may occasionally contain a small but detectable fraction of high molecular weight material as shown in Figure 1. Such a "double molecular weight impurity" has been observed previously in homopolymers and copolymers prepared with initiators such as **1**[20] and has been explained in terms of coupling of polymer chains.[21] The spectra (UV−vis, IR, and ^{1}H and ^{13}C NMR) of these blocks resemble a superposition of two homopolymers in ratios determined by stoichiometry.

We have taken advantage of the slow propagation of **2** and the subsequent secondary metathesis processes to prepare random copolymers of **2** with NBE. When a mixture containing 100 equiv of NBE and 10 equiv of **2** is reacted for 15 min with **1** in C_6D_6, only polyNBE, containing an initial 6.5:1 *cis*-olefin:*trans*-olefin ratio, along with unreacted **2**, is observed by ^{1}H NMR spectroscopy (Figure 2a). Subsequent ring-opening of **2** proceeds over a period of 5 h (Figure 2b), at which point the polyNBE still retains its kinetically determined stereocomposition. The signals assignable to the ring-opened product of **2** are identical to those present in poly**2**, and therefore, it is safe to assume that after 5 h substantial "blockiness" exists in this copolymer. Further reaction takes place, albeit slowly, and after 36 h no resonances from poly**2** segments are observable while over the same period the isomeric composition in polyNBE has approached the more thermodynamically consistent *cis*:*trans* ratio of 1:3.5 (Figure 2c). Additionally, two new resonances appear in the olefinic region at 6.38 (d) ppm and 6.13 (dd) ppm assigned to the new *trans*-phenylcyclopentyl repeat unit that arises as a consequence of statistical mixing between the polymer olefins with the still reactive metal site (Scheme 1). After quenching and isolation, the M_w/M_n (M_w = weight average molecular weight; M_n = number average molecular weight; M_w/M_n = polydispersity = PDI) values of these random copolymers averaged 2.0.

Other derivatives of **2** polymerize in a similar living and *cis*-specific fashion. We have reported the synthesis of 9-[(*tert*-butyldimethylsilyl)oxy][2.2]paracyclophan-1-ene (**3** in eq 2), its polymerization to *cis*-poly**3** using **1**, and the conversion of poly**3** to PPV. Although preparation of **3** requires two additional steps relative to **2**, the yield is higher (25% overall yield from commercially available paracyclophane) and purification is straightforward. There is negligible interference from the bulky silyl ether on the propagation process that occurs with a rate and specificity similar to those for **2**. The bulky OTBS functionality significantly enhances the polymer's solubility relative to poly**2**, and no precipitation has been observed even after exhaustive photolysis. It is possible to catalyze the *cis*-

---

[20] Saunders, R. S.; Cohen, R. E.; Schrock, R. R. *Macromolecules* **1991**, *24*, 5599.

[21] Feast, W. J.; Gibson, V. C.; Khosravi, E.; Marshall, E. L.; Mitchell, J. P. *Polymer* **1992**, *33*, 872.

Scheme 1

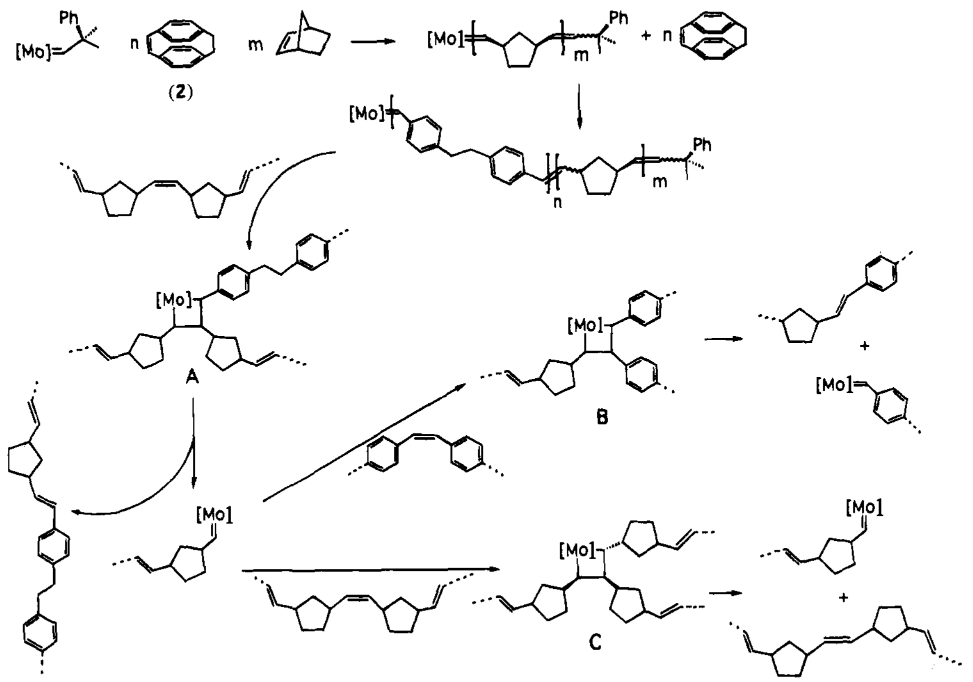

to *trans*-olefin isomerization in poly**3** (as well as poly**2**) by adding a catalytic amount of iodine (eq 3)at room temperature

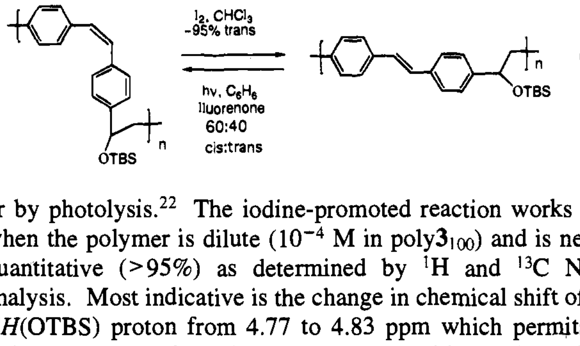

(3)

or by photolysis.[22] The iodine-promoted reaction works best when the polymer is dilute (10^{-4} M in poly$\mathbf{3}_{100}$) and is nearly quantitative (>95%) as determined by ^{1}H and ^{13}C NMR analysis. Most indicative is the change in chemical shift of the C*H*(OTBS) proton from 4.77 to 4.83 ppm which permits an estimate of the polymer's isomeric composition. Similarly, a significant shift of the olefinic resonances is observed from 6.50 to 7.12 ppm, although the latter is partly obscured by aromatic resonances. We have also found that *cis* linkages can be regenerated to an extent of 60% by photolyzing the *all-trans*-polymer in benzene using fluorenone as the photosensitizer. Starting with the *all-cis*-polymer, a similar final ratio of 60:40 is observed, and therefore we are confident that this is the photostationary equilibrium value. Therefore, both stereoregular forms are available as well as chemical and reversible photochemical means to tailor the percentage of each in a stereorandom form. Access to these materials will be useful when we address the effect of isomeric composition on bulk photophysics (*vide infra*).

To further probe the influence of monomer substituents on the polymerization reaction and ultimately bulk properties of isolated polymers, 9-(*n*-butyl)-9-[(*tert*-butyldimethylsilyl)oxy]-[2.2]paracyclophan-1-ene (**4**) was synthesized using an approach similar to that for preparing **3** (eq 4). Reaction of previously

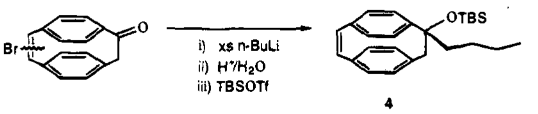

(4)

reported 9(10)-bromo[2.2]paracyclophan-9-en-1-one with excess *n*-butyllithium (3–4 equiv) in diethyl ether at −78 °C, followed by *in situ* quenching with water, generates 9-(*n*-butyl)-9-hydroxy[2.2]paracyclophan-1-ene which can be converted to **4** using *tert*-butyldimethylsilyl triflate and 2,6-lutidine. To obtain **4** pure enough for polymerization studies, it was chromatographed over silica gel using hexane and finally placed under vacuum overnight. The final yield of **4** from 9(10)-bromo[2.2]-paracyclophan-9-en-1-one is 75%.

Polymerization of **4** with **1** results in formation of *cis*-poly**4** with a random head-to-tail arrangement (eq 5). Again, the

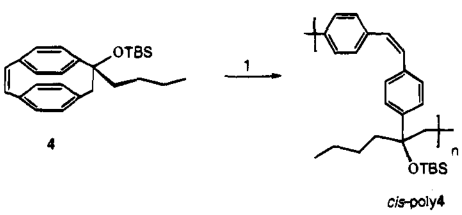

(5)

selectivity and activity for this reaction are similar to those originally observed for polymerization of either **2** or **3** with **1** as the initiator. It seems, therefore, that geminal disubstitution on a bridge site opposite the reactive olefin does not interfere with the polymerization sequence. As expected on the basis of the greater substitution, poly**4** shows enhanced solubility over poly**3**, especially in nonpolar solvents. Purification was typically carried out by precipitation upon adding a concentrated hexane solution to methanol.

Photocyclization of Poly3. One well-known photochemical transformation of *cis*-stilbene is its oxidative photocyclization to phenanthrene.[23] This two-step reaction proceeds first via generation of dihydrophenanthrene by a photochemically induced π^6 electrocyclic ring closure of the *cis* isomer and is then followed by oxidation. This second phenanthrene-forming step may be facilitated using a variety of reagents.[24] We have found that the stilbene components in poly**3** can be quantitatively

---

[22] Saltiel, J.; Ganapathy, S.; Werking, C. *J. Phys. Chem.* **1987**, *91*, 2755.

[23] Mallory, F. B.; Mallory, C. W. *Org. React.* **1984**, *30*, 1.

[24] (a) Liu, L.; Yang, B.; Katz, T. J.; Poindexter, M. K. *J. Org. Chem.* **1991**, *56*, 3769. (b) Saltiel, J.; Waller, A. A.; Sears, Jr., D. F. *J. Am. Chem. Soc.* **1993**, *115*, 2453. (c) Saltiel, J.; Waller, A. S.; Sears, Jr., D. F. *J. Photochem. Photobiol., A* **1992**, *65*, 29.

Table 2. Relationship among the Amount of I_2 Added to Poly3, M_n, and Phenanthrene Conversion[a]

amt I_2 (equiv)	% conversion[b]	M_n(calcd)	M_n(found)[c]	M_w/M_n
0	0	60 480	51 700	1.2
0.11	10	60 444	43 000	1.2
0.25	25	60 390	31 000	1.2
0.36	35	60 354	27 800	1.2
0.54	55	60 282	24 300	1.2
1.02	>95	60 120	20 300	1.2

[a] Typical reaction time of 4–5 h. [b] Determined by ^1H NMR spectroscopy. [c] GPC results versus polystyrene standards.

converted to phenanthrene by photolyzing dilute benzene solutions of poly**3** in the presence of a stoichiometric amount of iodine (relative to stilbene equivalents) and a large excess of propylene oxide. Iodine serves as the oxidant while propylene oxide consumes the hydrogen iodide formed during oxidation. These optimized conditions facilitate the rapid formation of disubstituted phenanthrene chromophores without intermolecular photodimerization (eq 6).

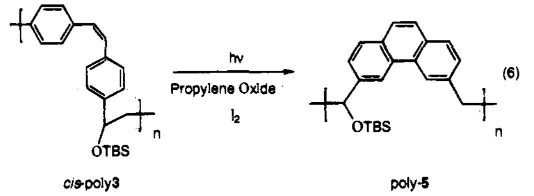

After workup and isolation, the extent of photochemical conversion in the resulting material can be determined by ^1H NMR spectroscopy. The ^1H and ^{13}C NMR spectra of pure poly**5** are characterized by broad and almost structureless signals, probably as a consequence of the decrease in motion enforced by the more rigid phenanthrene framework. Exceptions are provided by the signals at 3.25 and 5.15 ppm due to the diastereotopic methylene protons in poly**5** which are distinct and permit their integration relative to the analogous signals in *cis*- and *trans*-poly**3** in the regions of 2.9 and 4.8 ppm. In this way, the ratio of (both *cis* and *trans*) stilbene to phenanthrene units in the chain can be determined. There is a strict correlation between the amount of iodine added and the structural composition of the backbone (Table 2); for example, addition of 0.5 equiv of I_2 quickly produces a polymer composed of a randomly arranged and equimolar distribution of (predominantly *trans*) stilbene and phenanthrene units.

There is little change in the polydispersity value after photocyclization, indicating that the reaction is exclusively intramolecular in nature and that negligible degradation or chain cleavage occurs. However, a decrease in molecular weight[25] of 54% (poly**3**, M_n = 23 900; poly**5**, M_n = 11 100; see also Table 2) is observed by GPC after cyclization, indicating a smaller effective volume for poly**5** than poly**3** (Figure 3). The molecular weights determined by GPC depend on the extent of conversion (Figure 4), indicating that the polymer chains shrink substantially by this structural change. Additionally, block copolymers composed of polyNBE and poly**3** react similarly, *i.e.*, poly$\mathbf{3}_{12}$-*block*-polyNBE$_{120}$ is cleanly converted to poly$\mathbf{5}_{12}$-*block*-polyNBE$_{120}$ which is partially soluble in hexane.

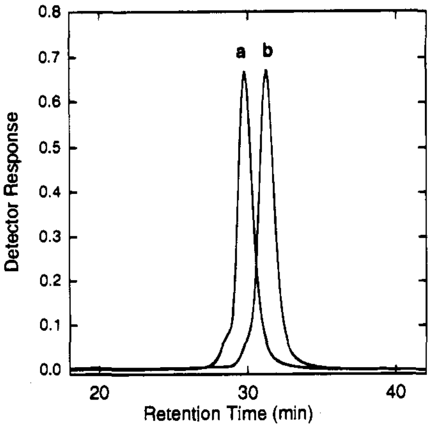

Figure 3. GPC elution curves of (a) poly$\mathbf{4}_{100}$ and (b) poly$\mathbf{5}_{100}$ derived from poly$\mathbf{4}_{100}$.

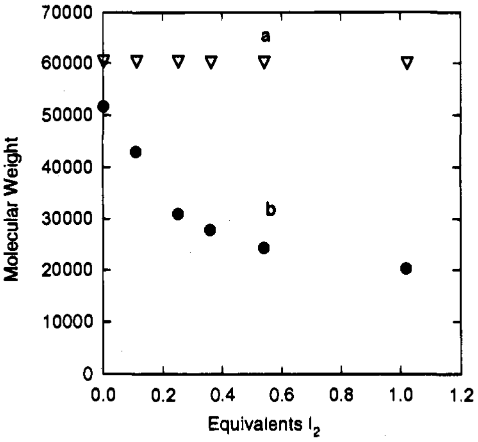

Figure 4. Volume contraction in the oxidative photocyclization of poly**4** to poly**5** measured as GPC-determined molecular weights loss: (a) calculated average molecular weight, (b) GPC-measured M_n.

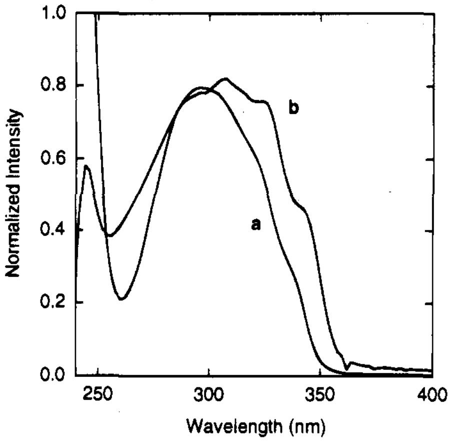

Figure 5. UV–vis absorption spectra of (a) fresh poly**2** and (b) irradiated poly**2**.

Absorption and Steady State Fluorescence Spectroscopy of Homopolymers and Copolymers. A noticeable red shift and emergence of fine structure occur in the absorption spectra of poly**2** upon irradiation (Figure 5). The broad, almost featureless, spectrum of fresh poly**2** closely resembles that of dialkyl-substituted *cis*-stilbenes,[26,27] except for broadening characteristic of polymeric samples. Likewise, the vibronically resolved spectrum of irradiated poly**2** matches well that of *trans*-dimethylstilbene. We are certain that the spectral change is due to a photoinduced *cis* to *trans* isomerization of many of the stilbene moieties. In the IR spectra, a decrease in signal intensity at 880 cm^{-1}, due to the out-of-plane vibration of the *cis*-vinylene

---

[25] All molecular weight determinations in this work were made using a GPC calibrated with commercial polystyrene standards. Therefore, these values are best regarded as "apparent" molecular weights.

[26] For a recent review of stilbene chemistry and photophysics see: Meier, H. *Angew. Chem., Int. Ed. Engl.* **1992**, *31*, 1399.

[27] Mooney, W. M.; Brown, P. E.; Russell, J. C.; Costa, S. B.; Pedersen, L. G.; Whitten, D. G. *J. Am. Chem. Soc.* **1984**, *106*, 5659.

[28] Saltiel, J.; Waller, A.; Sun, Y. P.; Sears, D. F. *J. Am. Chem. Soc.* **1990**, *112*, 4580.

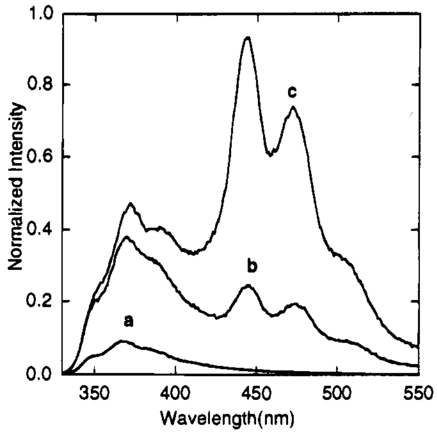

Figure 6. Dependence of fluorescence spectra ($\lambda_{\text{excitation}}$ = 330 nm) of poly**2** on irradiation time: (a) fresh polymer, (b) 2 min (c) 10 min.

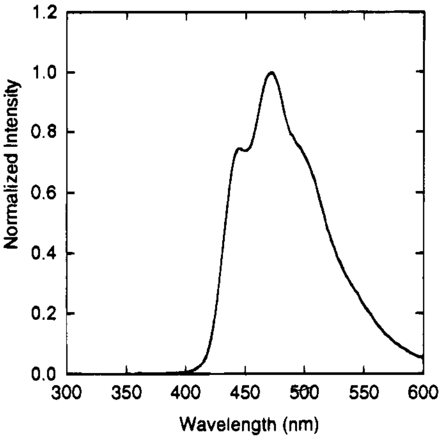

Figure 7. Fluorescence spectrum ($\lambda_{\text{excitation}}$ = 330 nm) from a thin film of poly**2** cast on quartz.

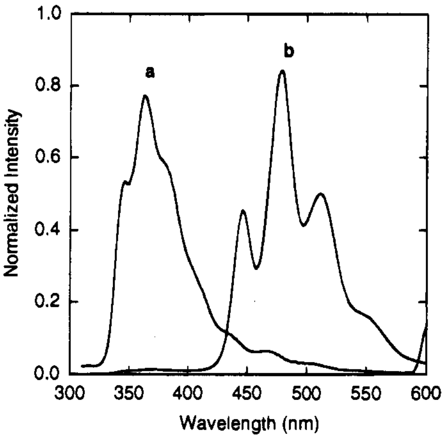

Figure 8. Normalized fluorescence spectra ($\lambda_{\text{excitation}}$ = 330 nm) of fully irradiated (a) random copolymer of NBE and **2** and (b) poly**2**$_{12}$-*block*-polyNBE$_{200}$.

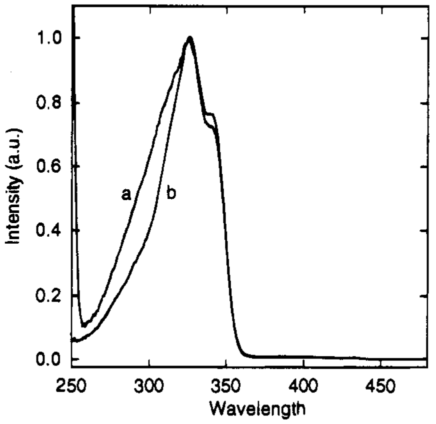

Figure 9. Normalized excitation spectra of poly**2**$_{12}$-*block*-polyNBE$_{200}$ monitored at (a) 375 nm and (b) 475 nm.

C–H bond, occurs simultaneously as the signal intensity of the *trans* isomer at 963 cm^{-1} intensifies.

The fluorescence of poly**2** changes also with irradiation, and this dependence is shown in Figure 6. The initial spectrum of freshly precipitated material is similar to that of *trans*-stilbene. Although the polymerization is ~98% *cis*-selective, fluorescence from primarily the *trans* isomer is observed because it is nearly 3 orders of magnitude more intense.[28] Following an initial exposure of 2 min, the *trans*-stilbene-like fluorescence increases substantially, but more importantly, a band that is significantly red-shifted begins to emerge (Figure 6). After 10 min of additional irradiation, this low-energy band becomes predominant, but subsequent analysis fails as the *trans* content increases to an extent that precipitation occurs. Films of poly**2**, easily cast onto quartz plates by slow evaporation of concentrated solutions, show only the low-energy fluorescence albeit less well vibronically defined (Figure 7).[29]

To circumvent solubility problems, the fluorescence characteristics of poly**2**$_{12}$-*block*-polyNBE$_{200}$ were measured. The covalent link between the large amorphous polyNBE chain and the smaller polychromophore segment maintains the material in solution, even after exhaustive photolysis. After 30 min of irradiation, the fluorescence of poly**2**$_{12}$-*block*-polyNBE$_{200}$ clearly shows nearly complete conversion to the low-energy component (spectrum b in Figure 8). Diluting solutions of poly**2**$_{12}$-*block*-polyNBE$_{200}$ effected no change in the ratio of the two bands. Emission from the random copolymer, under all conditions and sample history, is dominated by stilbene-like fluorescence (spectrum a in Figure 8). Therefore, even though the random copolymer is identical to poly**2**$_{12}$-*block*-polyNBE$_{200}$, at least with respect to the number and type of monomer constituents, the fluorescence of the latter has shifted bathochromically by approximately 100 nm (approximately 0.8 eV). Since the major structural difference between the two copolymers is a greater separation of the stilbene components in the random case, these results point to chromophore close proximity and, by inference, cooperativity as the origin of this dramatic red shift.

Excitation spectra provide complementary insight into the interactions of fluorescent chromophores in the ground and excited states.[30] Particularly impressive has been the application of such spectra to delineate the nature of pyrene interactions in polymeric assemblies.[1a] The steady state excitation spectra of poly**2**$_{10}$-*block*-polyNBE$_{150}$ in CHCl$_3$ detected at 375 and 480 nm are shown in Figure 9 (the sample was irradiated briefly so that the fluorescence at 480 nm was approximately 4 times as intense as that at 375 nm). Both excitation spectra closely match the absorption spectra of the stilbene components, and the only difference between them is the intensity on the high-energy side of the maximum. Similar results are obtained for poly**2**$_{100}$ in stages where both high- and low-energy components are observable regardless of the monitored wavelength. The shorter sequence of poly**2**$_{10}$-*block*-polyNBE$_{150}$ is significant in that the

---

(29) Suspensions of poly**2** can also be prepared using a tungsten initiator similar to **1**. This version of poly**2** is insoluble because of the poor *cis* selectivity of the tungsten-based propagating alkylidene. However, the intense blue fluorescence of this poly**2** suspension is identical to that of the film shown in Figure 10; see: McNamara, J. J.; Wudl, F. *Polym. Prepr.* **1993**, *34*, 528.

(30) Zagrobelny, J.; Betts, T. A.; Bright, F. V. *J. Am. Chem. Soc.* **1992**, *114*, 5249.

absence of any additional spectral features argues strongly against the presence of a more delocalized impurity (*vide infra*).

Poly**3** matches the photophysical behavior of poly**2** in several ways. Freshly isolated material shows stilbene-like fluorescence, but upon photolysis, the red-shifted, vibronically defined fluorescence appears. However, because all isomers of poly**3** are soluble, it is possible to study the effect of stereocomposition in homopolymers. Relative to poly**2**, the growth of the low-energy component in poly**3** is slower in a qualitative sense, and it is also ~12 nm blue-shifted. Upon irradiation, the intensity first maximizes and then decreases somewhat before reaching what appears to be a photostationary equilibrium. At this stage, the relative ratio of the two component bands is approximately 1:3 which is invariant over the concentration range 2.3×10^{-5} to 2.3×10^{-8} M (the most dilute measurement was dictated by the fluorimeter's sensitivity). In one experiment, the polymer solution was irradiated inside the fluorimeter using the excitation lamp until the low-energy intensity had maximized. Removal of solvent left poly**3** that, by ^{1}H NMR spectroscopy, contained approximately 75% *cis* linkages. Significantly, no low-energy fluorescence was observed in samples of *trans*-poly**3** prepared using the iodine-catalyzed isomerization, but it was reestablished by introducing *cis* linkages using the protocol shown in eq 3.[31] Therefore, both isomerically pure extremes are available, display only stilbene-like photophysics, and serve as starting templates into which the alternate isomer can be introduced with the aim of affecting secondary structure.

Fluorescence quantum yield determinations for poly**3** in chloroform were done using *trans*-stilbene as a standard.[32] Fresh samples of poly**3** were photolyzed with the excitation lamp in the sample holder of the fluorimeter until the overall fluorescence was maximized, and the quantum yield was determined at $\phi_f = 0.20$ ($\lambda_{exc} = 310$ nm). This efficiency represents roughly a 4-fold increase over that of *trans*-stilbene.[33] For comparison, solutions of *all-trans*-poly**3** were measured to have $\phi_f = 0.08$ using the same method.

Two block copolymers composed of a short segment of **3** and polyNBE$_{100}$ were prepared to probe the influence of chain length. Since Figure 8 already determines that a 12-monomer sequence imitates many of the homopolymer characteristics, the two blocks were made purposely short beginning with only 2 and 5 equiv of **3**. For practical purposes, these molecules may be seen as polyNBE containing a small number of stilbenes in sequence as end groups. Their preparations involved first reacting the appropriate amount of **3** with **1** over a period of 4−5 h, then adding 100 equiv of NBE, and finally quenching the reaction with benzaldehyde. The polyNBE$_{100}$ block in this case is attached to provide a handle for convenient purification (by precipitation) and to increase the overall mass. In this way, the troublesome difficulties associated with oligomer purification are avoided. The two block copolymers are tentatively assigned as poly**3**$_2$-*block*-polyNBE$_{100}$ and poly**3**$_5$-*block*-polyNBE$_{100}$ to reflect the relative ratios of monomer added to initiator. It is unlikely tht the degrees of polymerization in the poly**3** segments are centered around stoichiometrically determined values since their magnitude is small. Differences in the rate of initiation versus the rate of propagation, the latter being slower, will skew the average chain length toward higher values than the initial monomer to initiator ratio. We will return to this issue again, but what should be certain is that differences between these two polymers are due to the different lengths of the poly**3** segment. Analytical data (^{1}H and ^{13}C NMR) are consistent with the proposed composition, and GPC analysis using a UV−vis photodiode detector confirmed stilbene-like absorption throughout the entire molecular weight range.

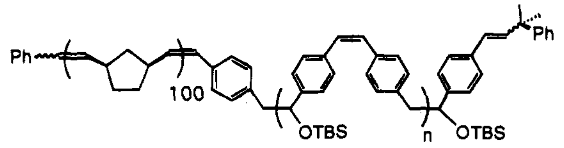

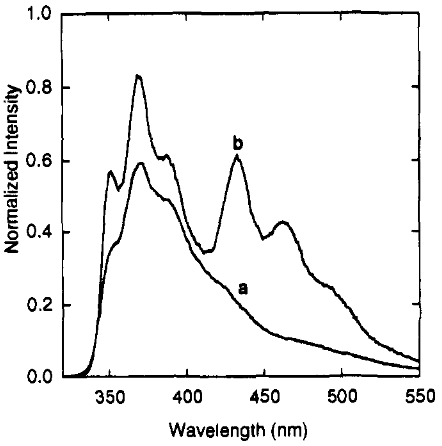

Figure 10. Normalized fluorescence spectra ($\lambda_{excitation} = 330$ nm, chloroform) of (a) poly**3**$_2$-*block*-polyNBE$_{100}$ and (b) poly**3**$_5$-*block*-polyNBE$_{100}$.

Fully irradiated poly**3**$_2$-*block*-polyNBE$_{100}$ and poly**3**$_5$-*block*-polyNBE$_{100}$ show significantly different fluorescence spectra (Figure 10). Poly**3**$_2$-*block*-polyNBE$_{100}$ resembles *trans*-stilbene spectroscopically regardless of concentration, solvent, or amount of preirradiation. Poly**3**$_5$-*block*-polyNBE$_{100}$ has characteristics very similar to those of the high molecular weight homopolymer. Excitation spectra for both samples were virtually identical and very similar to the stilbene-like absorption spectra shown in Figure 9. These results clearly underscore the importance of segment length on chromophore cooperativity.

Steady state fluorescence depolarization is often diagnostic of energy migration in polychromophores. The depolarization of the two fluorescent components of poly**3** was studied in different solvents. We obtained the degree of polarization (P) using the formula[34]

$$P = (I_\parallel - GI_\perp)/(I_\parallel + GI_\perp)$$

where $I_\parallel$ and $I_\perp$ refer to the intensities measured through a polarizer oriented parallel and horizontal to the polarization plane of the incident (excitation) beam. The correction factor G accounts for any possible instrument bias. Both the low-energy and high-energy bands of poly**3** in CHCl$_3$ show complete depolarization (*i.e.*, P approximately 0; see Table 3). In more viscous polyethylene glycol ($M_n \approx 550$), a medium wherein chain and molecular motions are dampened, the two components behave differently and the band at 355 nm retains some polarization. This polarization decreases slightly upon raising the temperature (refer to Table 3).

---

[31] Similarly, *trans*-poly**2**$_{12}$-*block*-polyNBE$_{200}$ also lacks a low-energy fluorescent component.

[32] Sharafy, S.; Muszkat, J. A. *J. Am. Chem. Soc.* **1971**, *93*, 4119.

[33] The quantum yield of *trans*-stilbene in nonpolar solvents has been reported to be in the 0.035−0.08 range. We have used a value of 0.049 from Saltiel, J.; Waller, A. S.; Sears, D. F.; Garrett, C. Z. *J. Phys. Chem.* **1993**, *97*, 2615. See also: Murov, S. L.; Carmichael, I.; Hug, G. L. *Handbook of Photochemistry*, 2nd ed.; Marcel Dekker: New York, 1993.

[34] Lakowicz, J. R. *Principles of Fluorescence Spectroscopy*; Plenum: New York, 1983.

[35] Because CHCl$_3$ and hexane differ in polarity, their respective solutions of poly**4** will differ in secondary structure, with the former keeping poly**4** in tighter coils and the latter permitting uncoiling and extension.

Table 3. Effect of Temperature and Solvent on Fluorescence Depolarization in Poly$\mathbf{3}_{100}$[a]

wavelength (nm)	CHCl$_3$	polyethylene glycol		
355	0.09[b]	0.20[b]	0.17 ± 0.02[c]	0.15[d]
375	0.08[b]	0.21[b]	0.18 ± 0.02[c]	0.15[d]
437	0.05[b]	0.05[b]	0.07 ± 0.02[c]	0.08[d]
508	0.07[b]	0.06[b]	0.04 ± 0.02[c]	0.05[d]

[a] Note: all spectra were excited at 270 nm. [b] Run at room temperature. [c] Run at 40 °C. [d] Run at 55 °C.

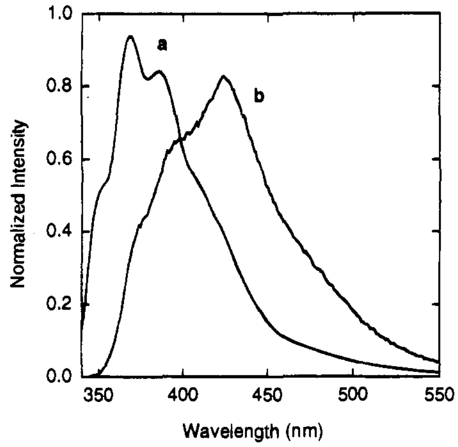

Figure 11. Fluorescence spectra ($\lambda_{\text{excitation}}$ = 300 nm) of (a) poly**4** in hexane and (b) a film of poly**4** on quartz.

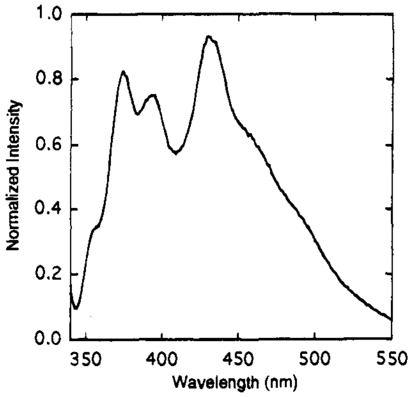

Figure 12. Fluorescence spectrum ($\lambda_{\text{excitation}}$ = 300 nm) of poly**4** in chloroform.

Poly**4** completes the series of polymers with increased backbone substitution. Fluorescence from a hexane solution is remarkably different from that of a film cast on a quartz plate from the same solution (Figure 11). Only stilbene-like fluorescence is observed in the former while the solid sample fluorescence is significantly red-shifted but not vibronically defined. In chloroform, a solvent that contracts coil dimensions for poly**4** more than hexane,[35] *both* components are observed, as shown in Figure 12, and their ratio is concentration independent.

The absorption and fluorescence spectra of poly**5** shown in Figure 13 differ little from the corresponding spectra of phenanthrene; the small red shifts of ~3–4 nm in absorption and ~10 nm in fluorescence can be attributed to 3,6-dialkyl substitution. Therefore, poly**5** behaves as a string of noninteracting chromophores despite their restricted separation. The fluorescence spectra of polymers of intermediate composition contain features similar to those of poly**3** and poly**5** in a ratio that depends on the extent of conversion. The effect of composition on fluorescence, while keeping $\lambda_{\text{excitation}}$ constant at 330 nm, is shown in Figure 14 (refer also to Figure 13). Note how the low-energy component decreases significantly as conversion to phenanthrene increases. Since the absorption maxima for stilbene and phenanthrene are sufficiently separated, it is possible in partially converted samples to excite selectively either chromophore by carefully choosing the excitation wavelength. Results of these experiments where a solution of a poly**3** converted to 65% stilbene and 35% phenanthrene units was excited at different wavelengths are shown in Figure 15. Only phenanthrene fluorescence is observed by excitation at 260 nm (spectrum a in Figure 15), while a spectrum showing combined phenanthrene and stilbene characteristics occurs with excitation

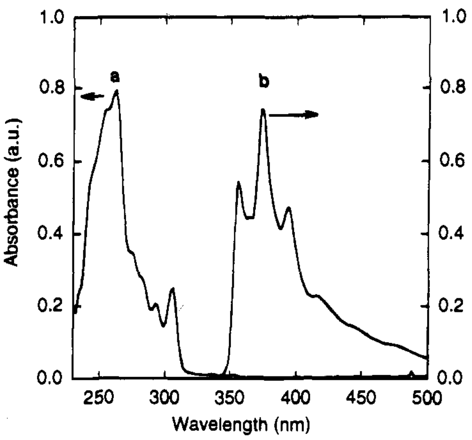

Figure 13. (a) Absorption and (b) fluorescence ($\lambda_{\text{excitation}}$ = 300 nm) spectra of poly**5** in chloroform.

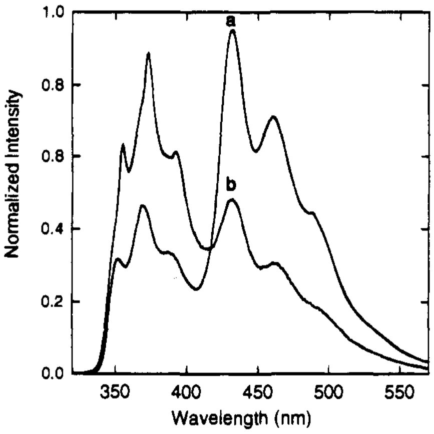

Figure 14. Effect of phenanthrene content on fluorescence spectra: (a) 0% conversion (pure poly**3**), (b) 25% conversion. For pure poly**5**, see spectrum b of Figure 13.

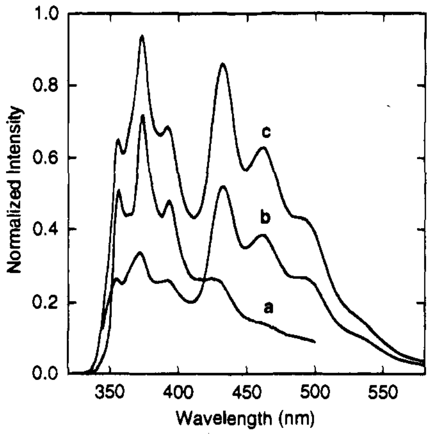

Figure 15. Dependence of the fluorescence spectra of partially converted (35% conversion) poly**5** on excitation wavelength: (a) $\lambda_{\text{excitation}}$ = 260 nm, (b) $\lambda_{\text{excitation}}$ = 330 nm, (c) $\lambda_{\text{excitation}}$ = 300 nm.

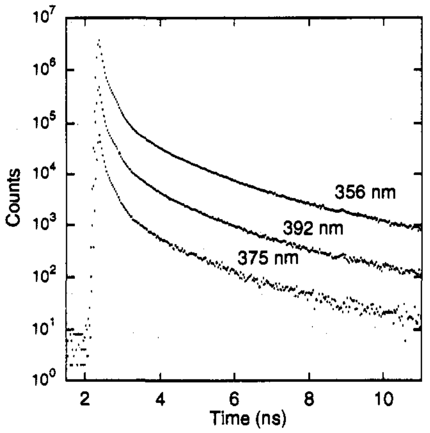

Figure 16. For poly**3** in $CHCl_3$, fluorescence lifetime measurements in the high-energy region of poly**3** in $CHCl_3$ monitored at different wavelengths.

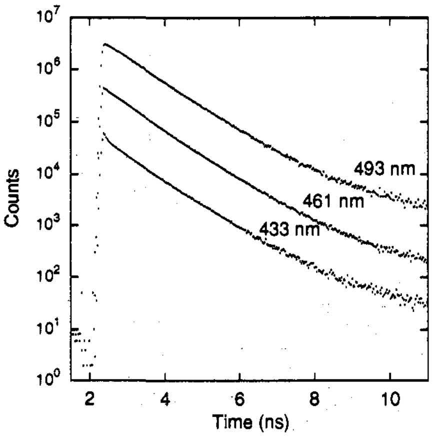

Figure 17. For poly**3** in $CHCl_3$, fluorescence lifetime measurements in the low-energy region as monitored at different wavelengths.

at 300 nm (spectrum c in Figure 15). At 330 nm, phenanthrene moieties do not absorb and fluorescence is strictly stilbene-like (spectrum b in Figure 15). These data are consistent with negligible interactions between the two types of chromophores.

Time-Resolved Fluorescence Spectroscopy. Time-correlated single photon counting measurements on a nanosecond time scale done on solutions of poly**2** and poly**3** reveal a faster intensity decay for the high-energy band (compare Figures 16 and 17 for poly$\mathbf{3}_{100}$). These measurements were carried out in chloroform where the absorbance at the exciting wavelength (300 nm) was standardized for all samples in the range of 0.1–0.3. No rising component was observed at 506 nm within the time domain of these experiments. Fitting the measured decay profiles required multiexponential functions, and some of these kinetic parameters are listed in Table 4. The high-energy envelope is dominated by a fast subnanosecond component and shows more heterogeneity, whereas the functional description of the low-energy side is close to monoexponential ($\tau \approx 1$ ns). The structured peaks within each band can be described by identical functions and thus are assigned to vibronic structure. This implies that there are only two distinct fluorescent species. Examination of the trace at 433 nm in Figure 17 (especially during the first 0.5 ns) reveals a slightly faster decay than for the traces at 461 and 493 nm, and we attribute this effect to spectral overlap with the tail end of the quickly decaying high-energy band.

By introducing phenanthrene progressively into poly**3**, the intensity decay profile at 375 nm shifts to longer lived regimes (Figure 18 and Table 5). Once poly**5** is obtained, the decay is for the first time monoexponential with $\tau = 6.3$ (curve c of Figure 18) and corresponds nicely to the lifetime obtained for phenanthrene ($\tau = 5.5$ ns) under similar conditions.[36] There is a strong but nonlinear correlation between the phenanthrene

Table 4. Parameters for Exponential Fits after Deconvolution from the Instrument Impulse Response for the Fluorescence Decay Curves of Poly**3** ($\lambda_{excitation} = 300$ nm) shown in Figures 16 and 17

λ_{em} (nm)	t_1[a] (ps)	A_1[a] (%)	t_2 (ps)	A_2 (%)	t_3 (ps)	A_3 (%)	t_4 (ps)	A_4 (%)	χ^2
356	58	53	520	9	1960	25	5730	13	1.068
369	84	68	528	22	2910	10			1.91
375	63	81	590	12	2290	7			1.11
392	98	14	883	83	2690	3			1.15
433	103	77	363	12	1320	9	4370	2	1.67
461	658	41	1020	58	4460	1			1.48
493	885	97	3020	3					1.74

[a] The table presents the results of four exponential fits to the luminescence decay. The values of t_{1-4} denote the time constants of the exponentials, and A_{1-4} denote their relative weights. The absence of entries for the higher variables means that an acceptable fit was obtained with two or three exponentials.

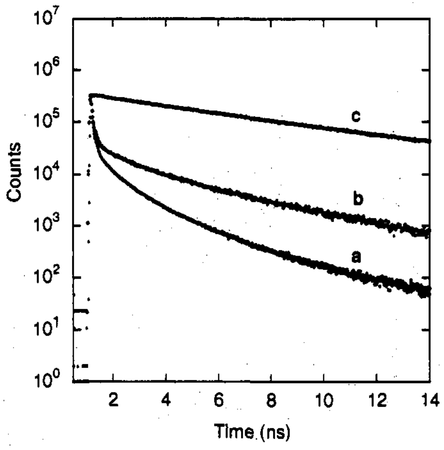

Figure 18. Effect of phenanthrene content on fluorescence decay curves for poly**3** in $CHCl_3$ at (a) 10% conversion, (b) 25% conversion, and (c) >98% conversion.

Table 5. For Polymers in Different Stages of Conversion from Poly**3** to Poly**5**, Exponential Fits to the Fluorescence Decay after Deconvolution from the Instrument Impulse Response ($\lambda_{excitation} =$ 300 nm)[a]

conversion (%)	λ_{em} (nm)	t_1 (ps)	A_1 (%)	t_2 (ps)	A_2 (%)	t_3 (ps)	A_3 (%)	t_4 (ps)	A_4 (%)	χ^2
10	356	62	59	1220	21	4330	20			2.22
	375	58	51	568	9	1950	26	5610	14	1.19
	392	60	51	538	10	1940	25	5690	14	1.24
	433	74	17	1060	68	4100	15			1.67
	461	93	5	1040	83	4190	12			1.63
	493	112	3	1050	85	4300	12			1.33
25	356	96	18	1150	26	4010	56			1.05
	375	98	18	1190	26	4130	56			1.08
	392	95	18	1150	28	4020	54			1.11
	433	403	42	1030	32	3790	26			1.22
	461	482	64	1360	20	3850	17			1.18
100	356	1400	3	6270	97					1.03
	375	1300	2	6330	98					1.09
	392	1410	4	6290	96					1.03
	433	940	17	5370	83					1.13
	461	885	17	4810	83					1.08

[a] The table presents the results of four exponential fits to the luminescence decay. The values of t_{1-4} denote the time constants of the exponentials, and A_{1-4} denote their relative weights. The absence of entries for the higher variables means that an acceptable fit was obtained with two or three exponentials.

---

(36) Encinas, M. V.; Rubio, M. A.; Lissi, E. A. *J. Photochem.* **1982**, *18*, 137.

content and the contribution from the longer lived component to the overall decay process.

Discussion

Polychromophore construction using living ROMP methods opens the way to emissive materials wherein the number average of polymerization ($\bar{X}_n$) matches closely the initial monomer: initiator ratio and their incorporation into block copolymer structures. Measurements of k_p/k_i (where k_p and k_i are the rates of propagation and initiation, respectively) show that the rate of initiation is similar to the rate of propagation.[34] While the neophyl group in initiator **1** is sterically large and interferes with approach of the monomer to the metal site, the propagating end is a substituted benzylidene which is electronically deactivated, and accordingly, the two species have similar reactivity. Therefore, there is no runaway propagation or chain transfer on the time scale of the polymerization, and the PDI values of the isolated polymers are narrow, approaching those expected from a Poisson distribution.[37] In the cases where living oligomers are prepared and then blocked with norbornene, the molecular weights of the oligomers are expected to deviate more severely from a Poisson distribution, since any discrepancies between k_p and k_i ($k_i \approx (8-10)k_p$ for **2**)[12] increase their influence as the number of equivalents of monomer decreases. Notwithstanding any deviations from ideality, it is clear that variations in photophysical behavior between blocked oligomers, for example, fluorescence from poly$\mathbf{3}_2$-*block*-polyNBE$_{100}$ and poly$\mathbf{3}_5$-*block*-polyNBE$_{100}$ as shown in Figure 10, arise as a result of differences in the average length of their respective stilbene segments. The Wittig-like termination reaction completely removes the transition metal fragments from the organic polymer, and repeated precipitation into organic solvents assures that no residual molybdenum-containing impurities remain trapped within the polymer to interfere with photooptical measurements.

When NBE and **2** are added together to **1**, a series of sequential reactions occurs that ultimately leads to a random copolymer. The basic olefin–metal complex interactions are depicted in Scheme 1. The olefin in NBE is more accessible than that in **2** and is polymerized quickly over a period of no more than 10–15 min. Subsequently, **2** is ring-opened and incorporated onto the end of the polyNBE chain. During the propagation of **2**, negligible metathesis involving olefins from the predominantly *cis*-polyNBE takes place, and upon complete consumption of **2** the remaining structure is close to a block copolymer with a ^{1}H NMR spectrum containing signals from both poly**2** and polyNBE (spectrum b of Figure 2). From this point, several metathesis reactions occur between the metal center and the polymer olefins over the next 36 h that change both the propagating alkylidene and the final polymer structure. One such reaction results from inserting a polyNBE olefin into propagating of poly**2** via metallacyclobutane **A** in Scheme 1. This insertion generates a new alkylidene similar to that of living polyNBE and removes the poly**2** fragment from the metal. Similarly, the olefin in a *cis*-stilbene link can form metallacycle **B** which can break up to a substituted benzylidene analogous to living poly**2**. Both metallacycles **A** and **B** generate the *trans*-phenylcyclopentylolefin observed in the final product (spectrum c in Figure 2). Note that if the formation and breakup of **B** were to continue indefinitely, no stilbene chromophores would remain in the final structure. To prepare the sample used to measure the spectrum in Figure 2b, the reaction must be quenched when approximately 40% of the stilbene links remain intact. Finally, metallacycle **C** mediates the *cis* to *trans* change in polyNBE stereochemistry.

Poly**2**, poly**3**, and poly**4** provide a clear and systematic progression of increased polymer substitution for structural comparison. Increasing substitution diminishes the percentage weight of the polymer that is photoactive and affects not only bulk solubility but also photophysics (*vide infra*). Coupled to the control over chain length and substituent size is the availability of pure stereoregular forms for all polymers. For all monomers, kinetic preferences of the propagation mechanism produce greater than 95% *cis*-polymer. The other extreme, *all-trans*-polymer, is obtained by the I_2-catalyzed isomerization as shown in eq 3. Solution photolysis permits regulating the contribution of each isomer to the chain beginning from either of the stereoregular forms. Therefore, paracyclophan-1-ene polymerization is valuable not only as a source for conjugated polymers, as shown in eq 2, but because it provides an unusually well behaved set of materials whose architectures can be tailored with precise control.

The most noteworthy feature of poly**2**'s fluorescence is the vibronically-defined low-energy band that appears as the structure is photochemically altered from the stereoregular *all-cis* arrangement (Figure 6). The vibronic progression suggests a different mechanism from that of excimer-forming polymers.[38] In the latter, broad and featureless fluorescence is a consequence of a nonbinding (repulsive) ground state energy surface between two chromophores. The different behavior of the block copolymer and the random stilbene-containing polymers shown in Figure 8 implies that the new fluorescent species originates from chromophore close proximity. We will refer to the low-energy component in poly(paracyclophan-1-ene)s as "aggregate" fluorescence to emphasize its multichromophore nature (2 or greater) and to distinguish it from normal excimer fluorescence.[39]

Unlike poly**2** (spectrum b in Figure 8), poly**3** displays a small component of stilbene-like fluorescence under all conditions (spectrum a in Figure 14). These different behaviors are consistent with the notion of aggregation, or cooperativity, because increasing the size and amount of substituents discourages chromophore close proximity. Relative to poly**2**, the substituents of poly**3** not only increase steric interference but also extend the polymer chain in good solvents to expand polymer dimensions and to increase the average inter-stilbene distance. Importantly, because dilution of poly**3** solutions only decreases the intensity of the entire spectrum while keeping the ratio of the two bands constant, we can infer that aggregation is *strictly intramolecular*, *i.e.*, involves stilbene units from the same chain.[40]

Observation of aggregate fluorescence in poly$\mathbf{3}_5$-*block*-polyNBE$_{150}$ and poly$\mathbf{2}_{10}$-*block*-polyNBE$_{150}$ provides the strongest argument against an undetermined impurity as the source of this band. Because a second chromophore would have to be present in every chain (recall the intramolecular nature of this phenomenon), it would represent a significant percentage of the total emissive block and should therefore be observable by NMR, UV–vis, or IR spectroscopy. After exhaustive

---

(37) Gold has treated the problem of PDI dependence on variations of k_p/k_i and shown that deviations from Poisson behavior are small when this ratio is 10 or less. See: Gold, L. *J. Chem. Phys.* **1958**, *28*, 91.

(38) (a) Letsinger, R. L.; Wu, T. *J. Am. Chem. Soc.* **1995**, *117*, 7323. (b) Altomore, A.; Corbin, C.; Ciardelli, F.; Panstone, M.; Solaro, R.; Houben, J. L. *Macromolecules* **1985**, *18*, 729.

(39) For an excellent review of photochemical processes in aggregated structures see: Ramamurthy, V. *Photochemistry in Organized and Constrained Media*; VCH: New York, 1991.

(40) For similar studies involving water soluble polymers that include both hydrophobic and hydrophilic components see: Gravett, D. M.; Guillet, J. E. *Macromolecules* **1995**, *28*, 274.

analysis, we have not been able to detect any functionalities apart from stilbene and polynorbornene.

For purposes of comparison, it should be noted that an earlier report of the fluorescence of poly(*p*-xylylene) attributed the red-shifted fluorescence from this material to ground state complexes.[41] It has since been demonstrated that this fluorescence can be reasonably explained in terms of a small amount of unsaturation in the main chains whose origin can be traced to pyrolytic procedures in the polymerization process.[42] We are confident that a similar explanation does not apply to our results, not only because of the above arguments against contamination in our polymers, but also because synthetic control of our polymerization procedures prevents such unwanted side reactions.

The structures of poly$\mathbf{3}_5$-*block*-polyNBE$_{150}$ and poly$\mathbf{3}_2$-*block*-polyNBE$_{150}$ are similar except for the lengths of the fluorescent segments which are better viewed as terminal functionalities rather than as second blocks. Aggregate fluorescence is clearly observed in poly$\mathbf{3}_5$-*block*-polyNBE$_{150}$, while stilbene-like fluorescence dominates almost exclusively in poly$\mathbf{3}_2$-*block*-polyNBE$_{150}$. Therefore, not only is close proximity of chromophores required, but a minimum number in sequence, we estimate in the range three to five, is necessary to allow suitable conformations that lead to aggregate formation. Perhaps it is at this stage that secondary structure effects create the necessary local conformations required by the aggregate sites. Further evidence of the modulation of fluorescence by secondary structure is provided by examining the effects of stereocomposition. Neither the pure *all-cis* nor *all-trans* forms form aggregates. It appears that only in the cases where a mixture of isomers is present are the required spatial geometrical arrangements satisfied. Tacticity effects on chromophore interactions in polymers have precedent; for example, as a result of a more ordered structure, excimer formation is more favored in isotactic polystyrene than in atactic polystyrene.[43] However, only in the case of the poly(paracyclophan-1-ene)s is vibronic structure observed, and this suggests stronger interchromophore binding.

The distinction between *trans*-stilbene aggregates in surfactant assemblies[27] and the mixed stilbene aggregates in our polymers should be noted. No photoconversion is required in the surfactant assemblies in order to record their aggregate spectra since they are specifically designed and fabricated to have a preordered structure by Langmuir–Blodgett techniques. In poly(paracyclophan-1-ene)s aggregation occurs accidentally, when many different environments are sampled in a stereochemically complex and irregular, secondary structure. Furthermore, the respective absorption and fluorescence spectra in the two systems are clearly distinct. Compared with the surfactant assemblies, we see no altered and blue-shifted absorption, but both aggregate fluorescence spectra show vibronic structure.

Many details of polymer photoprocesses have been delineated from studies of excimer formation and dynamics; relevant to our discussion is that excimer sites are typically created as a result of bond rotations rather than mass diffusion and that these sites behave as effective quenchers of monomer fluorescence via energy migration mechanisms. In poly(paracyclophan-1-ene)s, by analogy, only a minority of main-chain stilbenes may participate in aggregate formation, but they dominate spectral features because their excited states are populated via excitation migration. The most compelling evidence for this process is provided by the excitation spectra of the aggregate and the extremely fast decay of the stilbene-like fluorescence (Figure 16). The former matches the stilbene absorption spectrum, whereas the latter is consistent with energy transfer to the aggregate on a subnanosecond time scale. Similar energy transfer processes are well documented in aromatic vinyl polymers where aromatic chromophores are initially photoexcited and subsequently transfer this excitation to more stable excimer sites.[1,3] An excimer site is a mobile trap whose formation and, therefore, location depend on the local motion of chromophore side groups. Transfer of excitation energy can occur in solvated systems or between adjacent polymer chains in the bulk and rules out relating the intensities of fluorescence to concentration. Similarly, because no solvent exists between chains in the solid, the average interchromophore distance is minimized, energy migration is maximized, and total quenching of the high-energy component occurs. For these reasons, solid state samples are characterized by only aggregate fluorescence (Figure 7).

Fluorescence depolarization can in principle detect energy transfer. A chromophore that has not significantly changed its orientation (*i.e.*, by rotational motion) between the time of absorption and fluorescence will retain some polarization relative to the exciting polarized light. In an assembly where several energy transfer steps have occurred prior to fluorescence, the emitted light will be depolarized since each individual migration somewhat alters the original polarization. Poly**3**, with two different and clearly accessible bands, is an ideal candidate to detect selective depolarization. The experiments were made in dilute solutions where we have observed minimum interchain contacts within the lifetime of the fluorescence process and, therefore, probe strictly intrachain interactions, either between adjacent sites or across loops that bring chromophores near each other. Both bands in the fluorescence spectrum of poly**3** are mostly depolarized ($P = 0.09 \pm 0.02$) in chloroform, but by switching to more viscous polyethylene glycol as solvent the "monomeric" fluorescence retains more polarization ($P = 0.20 \pm 0.02$). Polarization data are listed in Table 3. The role of viscosity and the different extents to which the two energy bands scramble polarized exciting light are not straightforward to rationalize. In chloroform, total scrambling may be a result of fast chain dynamics and rotational motion that change the orientation of absorbing and emitting sites. Increasing viscosity slows down the rate at which an excited stilbene changes its orientation in space by increasing the drag on the moving sections of the polymer and decreasing the tumbling rate of the entire chain. Under these conditions, excited chromophores will then fluoresce with some of the initial polarization sustained only in the absence of energy transfer. To explain the experimental results in Table 3 and the fact that both bands are observed for poly**3**, we identify two independent factors: energy transfer and aggregate formation. The aggregation sites behave as low-energy traps for monomer excitation and are present in both viscous and nonviscous solvents. However, not all stilbene moieties participate in aggregate formation, and on the basis of the depolarization data, some stilbenes are not capable of transferring their excitation. These latter chromophores will contribute to the high-energy component and may be situated in parts of the polymer that restrict them from coming into close proximity with other chromophores.

Quantitative photochemical transformations of a polymer backbone such as that of poly**3** to poly**5** are rare. Further elaboration of this approach may offer a means to access phenanthrene-containing macromolecules or other fluorescent materials that are typically difficult to prepare.[44,45] GPC data

---

[41] Takai, Y.; Calderwood, J. H.; Allen, N. S. *Makromol. Chem., Rapid Commun.* **1980**, *1*, 17.

[42] Kochi, M.; Oguro, K.; Mita, I. *Eur. Polym. J.* **1988**, *24*, 917.

[43] David, C.; Putman de Lavarielle, N. Geuskens, G. *Eur. Polym. J.* **1974**, *10*, 617.

show not only that the reaction proceeds without cross-linking but that the chemical change shrinks considerably the extended volume occupied by the polymer chain. Compared to poly**3**, the two phenyl rings are locked in a cisoid arrangement, and their rotational motion relative to each other is eliminated. Consequently, some degrees of freedom are removed and the hydrodynamic volume occupied is diminished. Similar cyclization-induced volume contractions have been observed previously.[46,47]

By introducing phenanthrene functionalities into poly**3**, the polymer chain is "contaminated" with stereochemically rigid chromophores that show no evidence for interacting with each other. At the structural extreme of poly**5**, no aggregate formation occurs despite the contraction in dimensions, and fluorescence decay can be described well by a monoexponential fit that resembles closely that of phenanthrene itself. Other studies of phenanthrene-containing polymers have shown that this chromophore does not associate strongly; for example, it does not form excimers, whereas structural analogs containing naphthalene do.[48−50] Further, there is no indication that energy transfer from phenanthrene occurs to either stilbenes or aggregate sites. In samples of intermediate conversion, only phenanthrene fluorescence is observed upon excitation at 260 nm (spectrum a of Figure 15), and the long-lived component in the fluorescence decay profiles increases as the conversion percentage increases (Figure 18). Clearly, aggregation not only is a function of interchromophore distance and secondary structure but is dependent on the characteristics of the constituent chromophores.

Conclusion and Summary

More must be said with respect to possible degradation or decomposition to a more delocalized species, for example, dehydrogenation across a saturated linker. While no single piece of evidence can unequivocally eliminate this possibility, the *accumulated* body of information argues strongly against it. Most compelling is the lack of evidence for a more delocalized skeleton as measured by solution NMR, UV−vis absorption spectra, and, especially, the excitation spectra of short oligomeric species such as poly$\mathbf{2}_{10}$-*block*-polyNBE$_{200}$ and poly$\mathbf{3}_5$-*block*-polyNBE$_{150}$. Because aggregate fluorescence is concentration independent, we can safely rule out interchain interactions. Therefore, it is highly unlikely that unwanted chromophores exist as impurities because they would have to be present in every chain and thus comprise a significant percentage of the total fluorescent component. Further, because fluorescence of poly$\mathbf{3}_2$-*block*-polyNBE$_{150}$ is stilbene-like while poly$\mathbf{3}_5$-*block*-polyNBE$_{150}$ has a strong aggregate component, it is not likely that this fluorescence is attributed to stilbene decomposition since using such a reaction should not be chain length dependent.

Additional studies are required to set up structure−property relationships that enable formulation of aggregated polychromophores. Ultimately, by controlling through-space cooperativity, it would be useful for certain technological applications to direct aggregate fluorescence into the blue or near-ultraviolet spectral regions. Attaining this goal appears not to be easy. The lessons learned from the poly(paracyclophan-1-ene)s imply that aggregate formation will be rather elusive since its formation critically depends on the solvent, type of chromophore, and chain length. The different behavior of poly**2** and poly**4** shows how increasing substitution effectively separates interacting photoactive groups. Additionally and most importantly, stereochemistry and, therefore, secondary structure must be optimized. In our case, stereoregular polymers are not preferred but rather a disordered structure is favored most likely because it permits the polymers to sample a wider range of geometries.

The exact nature (*i.e.*, number of chromophores and geometry) of the aggregate remains at the present time undefined. It is not clear whether it is a pair of strongly interacting stilbenes in which the ground state is in a local minimum enforced by chain conformation or an ensemble of chromophores as is the case of aggregated stilbenes in Langmuir−Blodgett films. We are beginning molecular mechanics simulations of short oligomeric units with the goal of obtaining a clearer picture of the coil shape and relative orientation of chromophores. Stereochemical disorder requires us to model many different isomeric possibilities even in short chains and makes modeling nontrivial.

Pendant chromophores (structure **I**, **C*** = chromophore) reveal their cooperativity in the form of excimer fluorescence.[1a] The flexible three-carbon link assists by restraining the relative distances and orientation of **C*** so that dimerization can take place within the lifetime of the excited state. However, under all conditions the ground state will be repulsive. For main-chain polychromophores (structures **II**), interaction between **C***s is coupled more strongly to chain motions and secondary structure, and as a result, **C***−**C*** aggregation may be organized at a local conformational minimum that is robust on the time scale of emission. What is unique about poly(paracyclophan-1-ene)s is the high ratio of **C*** to total polymer mass. Typically, a long tether required for solubility reasons decreases the **C*** to total polymer mass ratio; when no tether is present, one obtains insoluble and intractable conjugated materials. In view of the acute dependence on coil dimensions and increased substitution (*i.e.*, poly**2** vs poly**4**), it is clear that similar aggregation will be observed only in unusually high chromophore content materials, and we are currently exploiting this guideline to prepare polymers that show analogous aggregate behavior.[51]

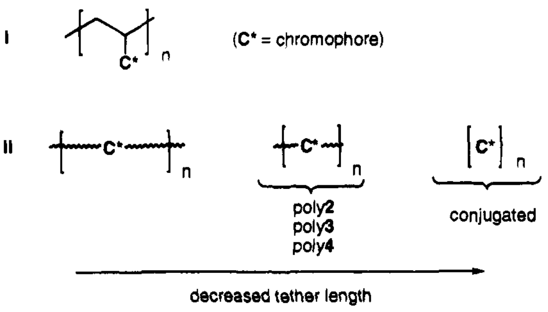

Experimental Section

General Details. All manipulations involving organometallic reagents were carried out using either high-vacuum or glovebox techniques as described previously.[52] ^{1}H and ^{13}C NMR spectra were

---

(44) Stenger-Smith, J. D.; Lenz, R. W.; Enkelmann, V.; Wegner, G. *Makromol. Chem.* **1989**, *190*, 2995.

(45) Capistran, J. D.; Gagnon, D. R.; Antoun, S.; Lenz, R. W.; Karasz, F. E. *Polym. Prepr. (Am. Chem. Soc., Div. Polym. Chem.)* **1984**, *25*, 282.

(46) Zhang, C.; Wang, Z. Y. *Macromolecules* **1993**, *26*, 3330.

(47) Goldfinger, M. B.; Swagger, T. M. *J. Am. Chem. Soc.* **1994**, *116*, 7895.

(48) Ng, D.; Guillet, J. E. *Macromolecules* **1982**, *15*, 724.

(49) Ng, D.; Guillet, J. E. *Macromolecules* **1982**, *15*, 728.

(50) Excimer emission has been detected in molecules that link two phenanthrene chromophores. See: Zachariasse, K. A.; Busse, R.; Schrader, U.; Kühnle, W. *Chem. Phys. Lett.* **1982**, *89*, 303.

(51) For example, polymers of general formula (R = alkyl)

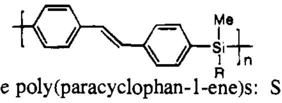

behave similarly to the poly(paracyclophan-1-ene)s: Sun, B. J.; Bazan, G. C. Unpublished results.

recorded on a Bruker AMX-400 NMR spectrometer at 400.1 and 100.6 MHz, respectively. Infrared spectra were recorded on a Perkin-Elmer 1600 FT-IR instrument, UV–vis absorption spectra on either a Perkin-Elmer Lambda 19 spectrophotometer or a Hewlett-Packard 8452A diode array spectrophotometer, and photoluminescence spectra on a Spex Fluorolog 2 spectrometer. An Osram 200-W high-pressure mercury arc lamp with collimated beam optics (Oriel Corp.) was used as the ultraviolet irradiation source. Time-correlated, single photon counting experiments were carried out on an instrument consisting of a mode-locked Nd:YLF laser (Quantronix) as the primary laser source and operating at 76 MHz. The second harmonic (KTP crystal) of the Nd:YLF laser was used to synchronously pump a dye laser (Coherent 700) with circulating Rhodamine 6G in ethylene glycol as the gain medium. As determined by autocorrelation, the pulse width of the dye laser was typically 8 ps and the laser was cavity dumped at a rate of 1.9 MHz. The dye laser was tuned to the desired wavelength for sample excitation. Fluorescence from the sample was collected by two convex lenses and focused at the entrance slit of a Spex 1681 monochromator (0.22 m) and was detected by a red-sensitive multichannel plate (MCP) detector (Hamamatsu R3809U-01). The single photon pulses from the MCP detector were amplified and used as the stop signal for a time-to-amplitude converter (TAC; EG&G Ortec), while the signal from a photodiode, detecting a small fraction of the dye laser output, was used as the start signal for the TAC. The start and stop signals for the TAC were conditioned before entering the TAC by passing through two separate channels of a constant fraction discriminator (CFD; Tennelec). The output of the TAC was connected to a multichannel analyzer (MCA) interface board (Norland 5000) installed inside a 486DX2 personal computer. The MCA was controlled by software from Edinburgh Instruments (Edinburgh, U.K.). The same software was used to carry out the deconvolution of the data and exponential fitting using the nonlinear least squares method. Solid state spectra of polymers were measured on films cast on quartz plates. Molecular weight determinations are relative to TSK polystyrene standards (Tosoh Corp.) and are based on separations by gel permeation chromatography (GPC) of chloroform solutions of the polymers in question; the standards ranged in molecular weight from 1051 to 1.9×10^5. The instrument employed was a Waters HPLC-GPC system equipped with a Model 600E controller and a Model 996 photodiode array detector and was loaded with Shodex columns (K-800P, 806, 804, 802, KF-801) arranged in series. The chloroform was Baker HPLC grade and was filtered through a Millex-SR 0.5-μm filter before use. High-resolution mass spectrometry was performed by the Midwest Center for Mass Spectrometry at the University of Nebraska—Lincoln. Toluene for polymerization was vacuum distilled from benzophenone ketyl immediately before use. Norbornene was distilled from Na/K alloy. The silica gel for column chromatography was 230–400 mesh and was purchased from EM Science. The initiator 1[53] and 9(10)-bromo[2.2]paracyclophan-9-en-1-one[54] were prepared according to literature procedures.

Synthesis of 1-(*n*-Butyl)[2.2]paracyclophan-9-en-1-ol. To a solution of 9(10)-bromo[2.2]paracyclophan-9-en-1-one (1.0 g, 3.4 mmol) in 60 mL of dry Et_2O at −78 °C was added 10 mL of *n*-BuLi (1.6 M solution in hexane) over a period of 30 min, and the mixture was stirred for another 30 min. The reaction mixture was quenched with 5 mL of deionized water at −78 °C and allowed to warm to room temperature. The resulting solution was washed with 30 mL of 1 M HCl, 30 mL of saturated NH_4Cl, 30 mL of brine, and finally 30 mL of deionized water. The organic layer was dried over $MgSO_4$ and filtered. The solvent was removed from the filtrate and dried overnight, giving 0.9 g (92%) of crude 1-(*n*-butyl)[2.2]paracyclophan-9-en-1-ol as a colorless liquid. The crude product was dissolved in hexane and absorbed on a column of 15 g of silica gel made up in hexane. Elution of the column with pure hexane provided 0.7 g (75%) or pure 1-(*n*-butyl)[2.2]paracyclophan-9-en-1-ol: ^{1}H NMR (400 MHz, $CDCl_3$) δ 0.98 (t, $J = 7.2$ Hz, CH_3, 3H), 1.47 (m, CH_2, 2H), 1.52 (m, CH_2, 2H), 2.10 (s, OH, 1H), 2.17 (m, CH_2, 2H), 2.90 (d, $J = 14.0$ Hz, CHH, 1H), 3.27 (d, $J = 13.9$ Hz, CHH, 1H), 6.34 (d, $J = 8.0$ Hz, CH, 1H), 6.38 (dd, $J = 5.2$, 1.7 Hz, C_6H_4, 2H), 6.54 (m, C_6H_4, 2H), 6.65 (d, $J = 8.1$ Hz, C_6H_4, 2H), 7.16 (dd, $J = 8.1$, 1.8 Hz, CH, 1H), 7.28 (d, $J = 2.5$ Hz, C_6H_4, 2H); $^{13}C\{^1H\}$ NMR (100 MHz, $CDCl_3$) δ 14.03 (CH_3), 23.05 (CH_2), 26.54 (CH_2), 42.05 (CH_2), 54.52 (CH_2), 82.78 (CH(OH)), 127.47, 128.00, 130.21, 130.50, 130.93, 131.61, 132.43, 132.50, 137.28, 137.53, 138.17, 138.35, 138.87, 142.75.

Synthesis of 9-(*n*-Butyl)-9-[(*tert*-butyldimethylsilyl)oxy][2.2]-paracyclophan-1-ene. To a solution of pure 1-(*n*-butyl)[2.2]paracyclophan-9-en-1-ol (0.8 g, 23 mmol) in 10 mL of dry CH_2Cl_2 at −30 °C were added 1.0 g (9.3 mmol) of 2,6-lutidine and TBSOTf (2.0 g, 7.6 mmol). The reaction mixture was allowed to warm slowly to room temperature and stirred for an additional 6 h. The resulting solution was washed with 10 mL of brine and 10 mL of deionized water. The organic layer was dried over $MgSO_4$ and filtered. The solvent was removed from the filtrate and dried overnight, giving about 1.1 g of crude 9-(*n*-butyl)-9-[(*tert*-butyldimethylsilyl)oxy][2.2]paracyclophan-1-ene as a colorless liquid. This liquid was dissolved in hexane and absorbed on a column of 15 g of silica gel made up in hexane. Elution of the column with pure hexane yielded about 1.1 g (90–99% depending on the reaction) of pure 9-(*n*-butyl)-9-[(*tert*-butyldimethylsilyl)oxy][2.2]paracyclophan-1-ene: ^{1}H NMR (400 MHz, $CDCl_3$) δ 0.33 (s, CH_3, 3H), 0.41 (s, CH_3, 3H), 0.91 (t, $J = 7.2$ Hz, CH_3, 3H), 1.10 (s, Si(CH_3)$_3$ 9H), 1.38 (m, CH_2, CH′H, 3H), 1.61 (m, CH′H, 1H), 2.17 (m, CH_2, 2H), 2.83 (d, $J = 14.1$ Hz, CHH, 1H), 3.45 (d, $J = 14.1$ Hz, CHH, 1H), 6.30 (m, 3H), 6.52 (m, C_6H_4, 2H), 6.57 (d, $J = 8.0$ Hz, 1H), 6.60 (d, $J = 8.4$ Hz, 1H), 7.21 (dm, $J = 8.2$ Hz, CH, 1H), 7.25 (s, C_6H_4, 2H); $^{13}C\{^1H\}$ NMR (100 MHz, $CDCl_3$) δ −1.95 (SiCH_3), −1.26 (SiCH_3), 14.10 (CH_3), 19.01 (SiC), 23.11 (CH_2), 26.40 (SiC(CH_3)$_3$), 27.19 (CH_2), 42.38 (CH_2), 54.91 (CH_2), 82.78 (CH(OTBS)), 127.62, 128.31, 130.12, 130.15, 131.24, 131.69, 132.53, 132.89, 137.46, 137.60, 137.73, 138.29, 138.90, 143.75; HRMS (EI) for $C_{26}H_{36}OSi$, *m/z* calcd 392.2535, found 392.2534.

Polymer Synthesis. Poly2. In a nitrogen-filled glovebox a round bottom flask was charged with **2** (400 mg, 1.94 mmol) and **1** (15 mg, 0.02 mmol), placed under vacuum, and dry toluene (40 mL) condensed at −78 °C. The resulting clear yellow solution was allowed to warm to room temperature and stirred for an additional 24 h in the dark. Quenching was accomplished by addition of 100 μL of dry benzaldehyde under an argon flow, and the mixture stirred for an additional 1 h. The product was purified by precipitation of a concentrated solution (15 mL) into pentane (250 mL). The resulting cream solids were isolated by centrifugation and placed under vacuum for several hours (yield 350 mg, 87%): $M_n = 26\,000$; PDI = 1.2; ^{1}H NMR (400 MHz, C_6D_6) δ 7.24 (d, $J = 8$ Hz, C_dH or C_cH, 4H), 6.83 (d, $J = 8$Hz, C_dH or C_cH, 4H), 6.50 (s, C_aH, 2H), 2.64 (s, C_fH, 4H); $^{13}C\{^1H\}$ NMR (100 MHz, $CDCl_3$) δ 140.5 (C_e), 134.9 (C_b), 129.6 (C_a), 128.7 (C_c or C_d), 126.4 (C_c or C_d), 37.4 (C_f). Assignment according to *cis*:

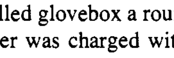

Poly3. In a nitrogen-filled glovebox a round bottom flask equipped with a vacuum line adapter was charged with **3** (336 mg, 1.0 mmol) and **1** (8 mg, 0.01 mmol). The apparatus was placed under vacuum, and dry toluene (25 mL) was condensed into the flask at −78 °C. The resulting light yellow solution was allowed to warm to room temperature and stirred for an additional 24 h. The reaction was quenched by addition of 50 μL of dry benzaldehyde under a counterflow of argon, stirred an additional 1 h, and concentrated to one-fourth of the original volume. The product was isolated by precipitation into 200 mL of MeOH and centrifugation. The resulting solids were redissolved in CH_2Cl_2, reprecipitated into 200 mL of MeOH, collected by centrifugation, and placed under vacuum for 24 h to yield 285 mg (85%) of poly**3**: $M_n = 23\,900$; PDI = 1.1; IR (KBr, thin film) ν_{max} (cm^{-1}) 3017, 2953, 2927, 2855, 1512, 1471, 1360, 1256, 1082, 934, 887, 834, 776; ^{1}H NMR (C_6D_6) δ 7.31–7.03 (8H, aromatic C-H's), 6.53 (2H, *cis*-olefin), 4.75 (1H, OCH), 2.87 (2H, benzylic CH_2), 0.93 (9H, C(CH_3)$_2$), 0.15 (6H, Si(CH_3)$_2$); $^{13}C\{^1H\}$ NMR (100 MHz, $CDCl_3$) δ 144.1, 137.9, 136.0, 135.1, 130.0, 128.5, 126.0, 125.8, 76.5, 47.5, 25.9, 17.9, −4.9, −5.1.

---

(52) Burger, B. J.; Bercaw, J. E. In *Experimental Organometallic Chemistry*; Wayda, A. L., Darensborug, M. Y., Eds.; ACS Symposium Series 357; American Chemical Society: Washington, DC, 1987.

(53) (a) Schrock, R. R.; Murdzek, J. S.; Bazan, G. C.; Robbins, J.; DiMare, M.; O'Regan, M. *J. Am. Chem. Soc.* **1990**, *112*, 3875. (b) Oskam, J. H.; Fox, H. H.; Yap, K. B.; McConville, D. H.; O'Dell, R.; Lichtenstein, B. J.; Schrock, R. R. *J. Organomet. Chem.* **1993**, *459*, 185.

(54) Stöbbe, M.; Reiser, O.; Näder, R.; de Meijere, A. *Chem. Ber.* **1987**, *120*, 1667.

Poly 4. The polymerization procedure similar was to that for poly**3**. Poly**4** was purified by precipitating concentrated hexane solutions into methanol (85% isolated yield): ^{1}H NMR (400 MHz, CDCl$_3$) δ 0.05 (SiCH_3, 6H), 0.81 (CH_3, 3H), 0.90 (SiC(CH_3)$_3$, 9H), 1.11 (CH′*H*, 1H), 1.22 (CH_2, 2H), 1.35 (C*H*′H, 1H), 1.76 (CH′*H*, 1H), 1.92 (C*H*′H, 1H), 2.93 (CH′*H*, 1H), 3.09 (C*H*′H, 1H), 6.45 (C*H*, 2H), 6.59 (C$_6H_4$, 2H), 6.97 (C$_6H_4$, 4H), 7.07 (C$_6H_4$, 2H); ^{13}C{^{1}H} NMR (100 MHz, CDCl$_3$) δ −2.0, −1.6, 14.2, 18.8, 23.1, 25.9, 26.3, 39.4, 50.7, 80.5, 80.6, 126.4, 127.9, 128.0, 129.6, 129.8, 130.4, 135.0, 135.3, 135.4, 136.3, 144.5.

Poly5. A solutiuon of poly**3** (44 mg, M_n = 23 900, PDI = 1.11) and I$_2$ (33.6 mg, 1.01 equiv) in 150 mL of benzene was degassed with argon for 30 min. Propylene oxide (10 mL, 0.14 mol) was then added followed by further argon degassing for an additional 20 min. The resulting solution was irradiated with a high-pressure mercury lamp for 4 h and the reaction monitored by either ^{1}H NMR spectroscopy or the disappearance of the characteristic iodine color. If excess iodine was present at the end of the reaction, workup included washing with 10% Na$_2$S$_2$O$_3$, water, and saturated brine followed by drying over MgSO$_4$. The solvent was removed *in vacuo* to give a light yellow solid and dissolved in 0.5 mL of CH$_2$Cl$_2$. This solution was precipitated into 100 mL of MeOH and centrifugated. Purification was achieved by reprecipitating a concentrated CH$_2$Cl$_2$ solution into methanol. Centrifugation and drying *in vacuo* overnight gave 43 mg (98%) of poly**5** as a pale yellow solid: M_n = 11 100; PDI = 1.10; IR (CH$_2$Cl$_2$, cm^{-1}) 3054, 2987, 2930, 2855, 1603, 1550, 1422, 1272, 1256, 1156, 1087, 1017, 987, 768, 718; ^{1}H NMR (400 MHz, CDCl$_3$) δ −0.31 (SiCH_3, 6H), 0.82 (SiC(CH_3)$_3$, 9H), 3.25 (CH_2, 2H), 5.15 (OC*H*, 1H), 7.66 (C$_6H_4$, 4H), 7.78 (C$_6H_4$, 2H), 8.52 (C$_6H_4$, 1H), 8.67 (C$_6H_4$, 1H); ^{13}C{^{1}H} NMR (100 MHz, CDCl$_3$) δ −5.1, −4.9, 18.2, 25.9, 48.6, 119.5, 123.8, 124.8, 126.1, 126.4, 128.1, 128.9, 130.0, 130.2, 130.7, 131.4, 137.1, 143.4.

***trans*-Poly3.** Poly**3** was dissolved in chloroform to obtain a 10^{-4} M solution. Treatment with a small amount of iodine for a period of 48 h at room temperature followed by solvent removal and a water rinse provides *trans*-poly**3** quantitatively. Polymer can be further purified by precipitating into hexane or methanol: ^{1}H NMR (CDCl$_3$) δ 7.44 (C$_6H_4$, 4H), 7.10 (C$_6H_4$ and C$_2H_2$, 6H), 4.77 (OC*H*, 1H), 2.88 (CH_2, 2H), 0.80 (SiC(CH_3)$_3$, 9H), −0.26 (Si(CH_3)$_2$, 6H); ^{13}C{^{1}H} (100 NMR, CDCl$_3$) δ 144.6, 138.2, 137.0, 135.4, 130.4, 128.3, 127.8, 76.4, 47.6, 29.7, 18.2, −4.99, −5.33; IR (KBr film, cm^{-1}) 3023, 2956, 2855, 1259, 1081, 1016, 962, 932, 886, 834.

Isomerization of *trans*-Poly3. A solution of *trans*-poly**3** (approximately 10 mg) in C$_6$H$_6$ (10 mL) containing fluorenone (approximately 2 mg) was introduced into a Schlenk flask and thoroughly degassed using argon. After 6 h of irradiation using a high-intensity UV lamp (365 nm), the solvent was removed and the *cis*:*trans* ratio determined by ^{1}H NMR spectroscopy (in CDCl$_3$) by measuring the relative intensities of the methylene peaks at 2.88 ppm (*trans*) and 2.82 ppm (*cis*). The polymer was purified for photophysical measurements by precipitation into pentane and collected by centrifugation.

Photoisomerization of *cis*-Poly3 Using Fluorenone as the Photosensitizer. *cis*-Poly**3** (12 mg) and fluorenone (2 mg) were dissolved in C$_6$H$_6$ (2−3 mL), and the solution was placed into a Schlenk flask. After three freeze−pump−thaw cycles, the flask was irradiated for 30 h. Removal of the solvent left behind a poly**3** with a *cis*:*trans* ratio of 60:40 (see above procedure).

Typical Block Copolymer Preparation. A round bottom flask with a needle valve adapter was charged inside the glovebox with **3** (48 mg, 0.143 mmol) and **1** (10 mg, 0.013 mmol). The assembly was attached to a high-vacuum line and dry toluene (15 mL) condensed over the reactants at −78 °C. The resulting clear yellow solution was allowed to warm to room temperature and stirred for an additional 6 h. A soltuion of NBE (250 mg, 2.6 mmol) in toluene (10 mL) was then added via syringe under vigorous stirring, and the mixture was stirred for 5−10 min. Active sites were quenched by addition of 50 μL of dry and oxygen-free benzaldehyde, and the solution was concentrated to one-third the original volume and precipitated into 150 mL of methanol. The product poly$\mathbf{3}_{10}$-*block*-polyNBE$_{200}$ appears as a white fibrous solid which is isolated by centrifugation and placed under vacuum overnight to remove residual solvent; yield 225 mg (85%), M_n = 23 600, PDI = 1.2. The spectra of block copolymers are a superimposition of the spectra of two component homoblocks in the appropriate ratio.

Acknowledgment. The authors gratefully acknowledge the NSF (Grant CHE-9120001) and the Center for Photoinduced Charge Transfer for support of this work. We thank Professor David Whitten and Dr. Samir Farid for helpful discussions, Drs. Stephen Atherton and Bradley Arnold for assistance with the fluorescence lifetime measurements, and the anonymous reviewers for their thoroughness and suggestions. Y.-J.M. thanks the Chemistry Department for a DeRight Fellowship.

JA951794Y